Arabidopsis GNARLED Encodes a *NAP125* Homolog that Positively Regulates *ARP2/3*

Salah El-Din El-Assal,[1,3] **Jie Le,**[1,3] **Dipanwita Basu,**[1]
Eileen L. Mallery,[1] **and Daniel B. Szymanski**[1,2,*]
[1]Agronomy Department
915 W. State Street
[2]Purdue Motility Group
Purdue University
Lilly Hall
915 W. State Street
West Lafayette, Indiana 47907

Summary

In migrating cells, the actin filament nucleation activity of ARP2/3 is an essential component of dynamic cell shape change and motility. In response to signals from the small GTPase Rac1, alterations in the composition [1] and/or subcellular localization [2, 3] of the WAVE complex lead to ARP2/3 activation. The human WAVE complex subunit, WAVE1/SCAR1, was first identified in *Dictyostelium* [4] and is a direct ARP2/3 activator [5]. In the absence of an intact WAVE complex, SCAR/WAVE protein is destabilized [6–8]. Although the composition of the five-subunit WAVE complex is well characterized, the means by which individual subunits and fully assembled WAVE complexes regulate ARP2/3 in vivo are unclear. The molecular genetics of trichome distortion in *Arabidopsis* is a powerful system to understand how signaling pathways and ARP2/3 control multicellular development [9–13]. In this paper we prove that the *GNARLED* gene encodes a homolog of the WAVE subunit NAP125. Despite the moderate level of amino acid identity between *Arabidopsis* and human NAP125, both homologs were functionally interchangeable in vivo and interacted physically with the putative *Arabidopsis* WAVE subunit ATSRA1. *gnarled* trichomes had nearly identical cell shape and actin cytoskeleton phenotypes when compared to ARP2/3 subunit mutants, suggesting that *GRL* positively regulates *ARP2/3*.

Results and Discussion

Arabidopsis trichomes are branched cells that are highly sensitized to mutations in cytoskeletal proteins. Trichomes are nonessential under laboratory growth conditions and present an ideal forward genetic inroad into morphogenesis. During trichome branch initiation, microtubules are required. Actin filaments function after branch formation and are needed to maintain polarized stalk and branch growth [14]. The "distorted group" of trichome morphology mutants consists of at least eight loci [15], and *gnarled* (*grl*), like all other distorted group mutants, is phenocopied by drugs that disrupt the actin cytoskeleton. The *grl* mutant was the subject of the original study that defined the stage-specific cell swell-

*Correspondence: dszyman@purdue.edu
[3]These authors contributed equally to this work.

ing and disorganized actin-based phenotypes of distorted mutants [16].

In a visual screen for distorted trichome mutants, we identified two new *grl* alleles and characterized four T-DNA insertion alleles (see below). Each of the six *grl* alleles described in this paper had indistinguishable stage-specific trichome swelling (Figure 1E) that did not occur in the wild-type (Figure 1A). Mature *grl* trichomes were swollen and twisted to variable degrees but consistently had a reduced branch length (Figure 1F, Table S1). The lobed shape of *grl* cotyledon pavement cells was indistinguishable from the wild-type (Figures 1C and 1G). However, the *grl* epidermis, like that of *distorted2* (*dis2* [*arpc2*]) had obvious cell-cell adhesion defects (Figure 1G, Table S1). Compared to the wild-type, the length of *grl* etiolated hypocotyls and individual hypocotyl cells was reduced significantly (Table S1). In three replicate trials, soil-grown, *grl* shoot fresh weight was reduced from 26% to 30%, relative to segregating wild-type controls (Table S1). Similar reductions in shoot fresh weight were observed with *grl-T2* and *grl-4* plants that were grown either in soil or tissue culture (data not shown). The overall architecture of *grl* plants (Figure 1H) did not differ from the wild-type (Figure 1D). The *grl* phenotypes are indistinguishable from those of *Arabidopsis ARP2/3* subunit mutants and suggest that *GRL* encodes either an ARP2/3 subunit or a positive regulator of ARP2/3.

In order to clone *GRL*, the gene was mapped to an 800 kb interval on chromosome 2 (Figure 2A). This region contained *AT2G35110* (*ATNAP125*), which encoded a homolog of the vertebrate WAVE complex subunit NAP125. To determine if *GRL* corresponded to *ATNAP125*, we sequenced the gene in the *grl-4* and *grl-6* backgrounds. Both alleles harbored mutations that truncated the predicted NAP125-like proteins (Figure 2B). We next tested the ability of the publicly available SALK T-DNA insertion lines [17] 135634 (*grl-T1*), 014298 (*grl-T2*), 038799 (*grl-T3*), and 009695 (*grl-T4*) to cause trichome distortion. Each T-DNA was located within the transcribed region of *ATNAP125*, caused the full array of *grl* phenotypes, and was allelic to *grl-6*. The series of *grl* T-DNA alleles is predicted to generate progressively truncated proteins, and in the case of *grl-T2*, we confirmed that the insertion caused premature termination of the *AT2G35110* transcript (data not shown). As a final test for gene identity we rescued the *grl* phenotype by overexpressing the full-length *ATNAP125* (GenBank accession number NM_129064) cDNA with the strong 35S viral promoter (see below). Taken together, these data prove that we have correctly identified the *GRL* gene, and we will refer to *ATNAP125* as *GRL* for the remainder of this paper.

We used RT-PCR to identify an unannotated intron in the 5′UTR of *GRL* and an in-frame stop codon upstream from the predicted start codon (GenBank accession number AY662956). The deduced 149 kDa GRL protein did not encode any recognizable domains but shared 22% amino acid sequence identity with human NAP125.
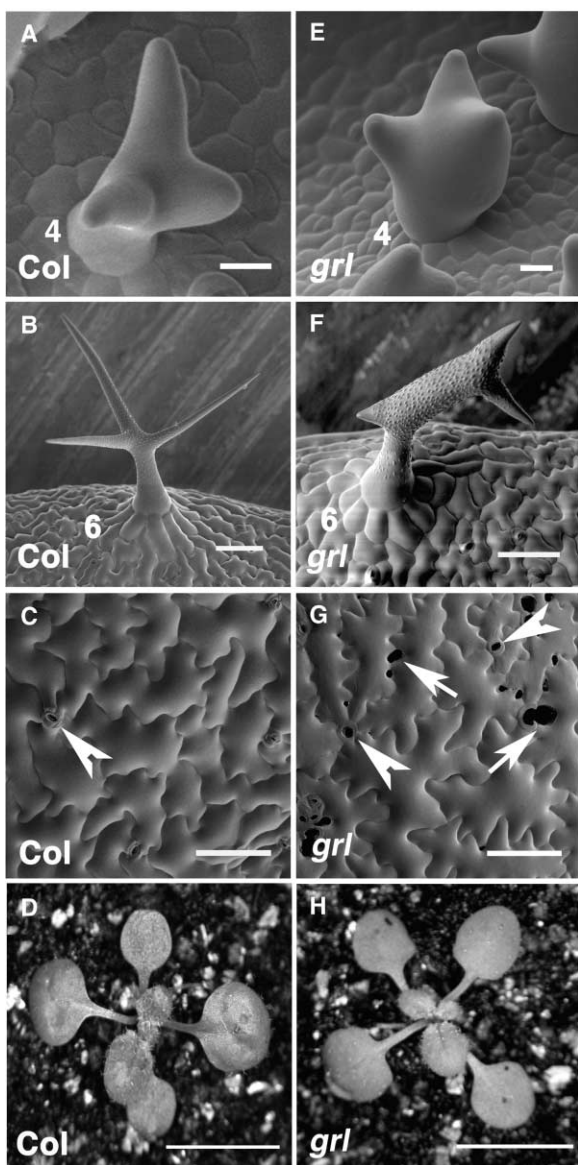
Figure 1. Trichome, Pavement Cell, and Whole-Plant Phenotypes of Wild-Type and *grl* Plants

(A and E) Scanning electron microscopy (SEM) images of stage-four wild-type (A) and *grl* trichomes (E). Stage-four cells have blunt branch tips and are at the transition to actin-dependent growth.
(B and F) SEM images of stage-six wild-type (B) and *grl* trichomes (F).
(C and G) SEM images of cotyledon epidermal pavement cells: wild-type (C) and *grl* (G) cotyledons. Images were taken from the upper cotyledon surface at 12 DAG.
(D and H) Wild-type (D) and *grl* (H) plants.
Scale bars: (A) and (E) = 10 μm, (B) and (F) = 50 μm, (C) and (G) = 100 μm, and (D) and (H) = 1 cm.
Wild-type is Col-0. Numbers in (A), (B), (E), and (F) indicate different developmental stage of trichomes. White arrows indicate gaps between adjacent pavement cells. White arrowheads indicate stomatal pores.

Figure 2. Mapping and Molecular Characterization of *GRL* Alleles

(A) The mapping interval of the *GRL* gene. The rectangles identify the relevant molecular markers and the oval indicates the *GRL*-containing BAC (T4C15). The recombination frequencies are shown for each marker.
(B) The physical structure of the *GRL* gene and the definition of *grl* alleles. The location and/or nature of the *grl-4*, *grl-6*, and the SALK T-DNA alleles, *grl-T1*, *grl-T2*, *grl-T3*, and *grl-T4* are labeled. Filled rectangles represent *GRL* exons. Open rectangles indicate the 5′ and 3′ UTRs. All alleles were generated in the Col-0 background. The molecular nature of each allele was determined by directly sequencing PCR products.

human homolog [1], is a subunit of a WAVE signaling complex. First we determined if putative *Arabidopsis* WAVE and ARP2/3 subunit genes were expressed coordinately in major plant organs. *Arabidopsis AT5G18410* (*ATSRA1*) is a single gene and encodes a homolog of the 140 kDa WAVE complex subunit PIR121 [1]. The founding member of the PIR121 family is SRA1 [18], and in this paper we will refer to the SRA1/PIR121 family members collectively as SRA1. *ATBRK1* encodes a homolog of the human WAVE complex subunit HSPC300 [1]. Maize *BRK1* encodes an HSPC300 homolog and is required for the crenulation of leaf epidermal cells [19]. We found no clear homologs of the WAVE complex subunits ABI2 or the ARP2/3 activator SCAR/WAVE in database searches. However, there are *Arabidopsis* proteins that share amino acid sequence homology with the domains of ABI2 and SCAR/WAVE that are needed for WAVE complex assembly [2]. The function of these candidate WAVE subunit-like genes is not known. RT-PCR experiments using RNA isolated from several major organs indicated that the WAVE complex homologs *GRL*, *ATSRA1*, and *ATBRK1* had expression patterns that resembled those of the ARP2/3 subunit genes *DIS2* (*ARPC2*) and *ATARPC4* but differed clearly from the *GAPC* reference gene (Figure 3). The expression pattern of *GRL* and *ARP2/3* subunits did not vary in cotyledons and leaves at different developmental stages (data not shown). These data are consistent with the idea that some type of plant WAVE complex exists.

If GRL functions as a subunit of a WAVE complex, a direct interaction with the SRA1 subunit is expected [2, 20]. Complexes containing SRA1 and NAP125 have been purified based on affinity for several signaling molecules [18, 21], and the interaction between SRA1 and NAP125 is thought to provide the physical link between upstream signals and altered WAVE complex activity [1, 2]. To test for a direct interaction between GRL and ATSRA1, full-length, tagged proteins were expressed in *E. coli* and

With the exception of small N- and C-terminal additions in GRL, a multiple sequence alignment of GRL and several known NAP125 homologs revealed uniform levels of identity along the entire length among the NAP125 family members (Figure S1).

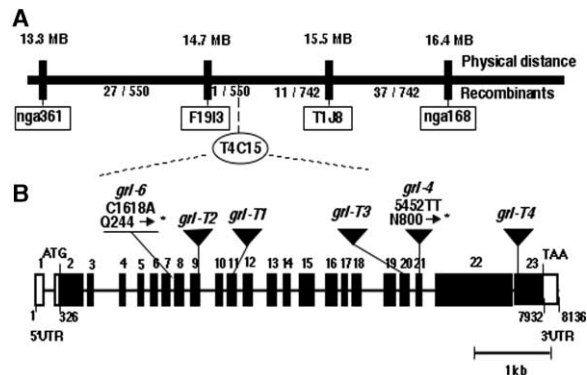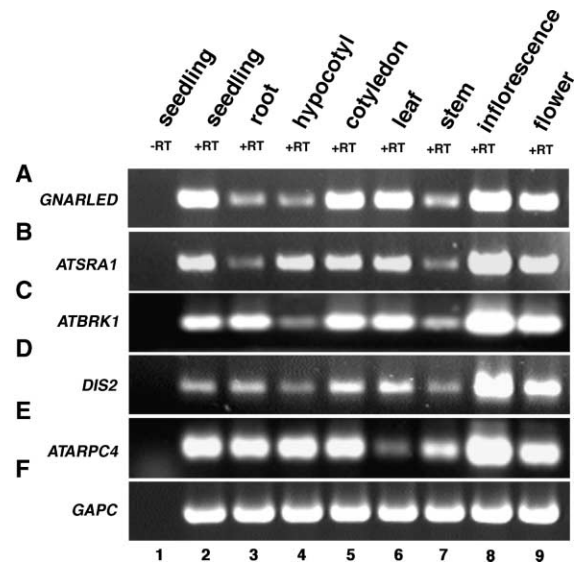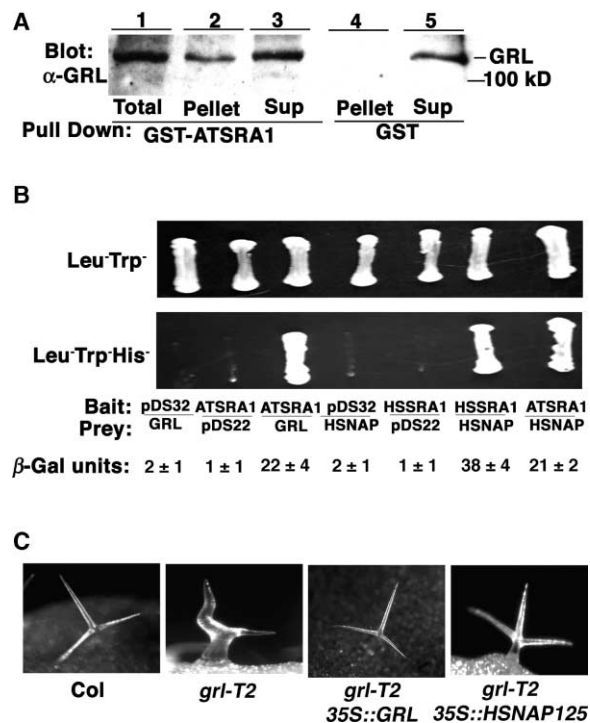We wanted to begin to test the idea that GRL, like its

Figure 3. The Expression Pattern of Putative Wave Complex Subunit Genes Overlaps with that of the ARP2/3 Subunit Genes

Total RNA isolated from the organs listed at the top of the figure was analyzed by RT-PCR by using gene-specific primers for *GNARLED, ATSRA1, ATBRK1*, and two representative ARP2/3 subunit genes. (A) *GRL*. (B) *ATSRA1*. (C) *ATBRK1*. (D) *DIS2* (*ATARPC2*). (E) *ATARPC4*. (F) *GAPC* (glyceraldehyde-3-phosphate dehydrogenase C subunit).
Lane 1, no reverse transcriptase (−RT) control; lanes 2–9, various RNA samples subjected to RT treatment. Control experiments that lacked RT were conducted on all RNA samples but only the seedling experiment is shown. For each primer pair, the PCR cycle number was optimized to reveal relative differences in expression between organs and did not exceed 20 cycles for any primer pair.

Figure 4. GRL and Human NAP125 Interact Physically with ATSRA1 and Have Interchangeable Functions In Vivo

(A) GRL and ATSRA1 physically interact in GST pull-down assays. Lanes 1–5, binding reactions were separated by SDS-PAGE and probed with an anti-GRL antibody; lane 1, 5% of total binding reaction; lane 2, GST-ATSRA1 bead bound pellet fraction; lane 3, unbound supernatant fraction; lanes 4, GST bead bound fraction; lane 5, unbound supernatant fraction. Full-length GRL and ATSRA1 were expressed in *E. coli* as N-terminal His and GST fusions, respectively. For detailed methods see Supplemental Data.
(B) Full-length GRL and human NAP125 interact with the *Arabidopsis* ATSRA1 in the yeast two-hybrid assay. The two-hybrid constructs and the β-galactosidase assay results for each strain are defined adjacent to the corresponding yeast patches. The constructs introduced into each strain are listed below the Leu− Trp− His− panel. Yeast two-hybrid interactions were analyzed based on growth on Leu− Trp− His− media (lower) and β-galactosidase activity. For detailed methods see Supplemental Data.
(C) Overexpression of *Arabidopsis* and human NAP125 homologs rescues *grl* trichome distortion. Panels from left to right: Mature Col-0 wild-type trichome, distorted *grl-T2* mature trichomes, rescue of the *grl* trichome distortion by *GRL* overexpression, and rescue of the *grl* trichome distortion by overexpression of human NAP125. NAP125 homologs were overexpressed in stably transformed lines by using the strong viral 35S promoter and the Gateway-compatible binary vector pGWB2 (a gift from T. Nagawa, Shiman University, Japan).

detected with an antibody that specifically recognized GRL (Figure S2). In GST pull-down assays, GST-tagged ATSRA1 interacted physically with full-length GRL (Figure 4A, lane 2). GRL did not interact with GST alone (Figure 4A, lane 4) or nonspecifically with large, His-tagged proteins because in control experiments ATSRA1 beads did not bind to an unrelated His-tagged 140 kDa protein (data not shown). Therefore the interaction between GRL and ATSRA1 is direct and specific.

We next tested whether the human NAP125 was capable of interacting with ATSRA1. WAVE subunits are not present in yeast, and the two-hybrid assay is a proven method to analyze WAVE subunit interactions [22]. Despite GRL and human NAP125 sharing only 22% identity, we detected a robust two-hybrid interaction between human NAP125 and ATSRA1 (Figure 4B, lower). We also detected a direct interaction between human NAP125 and SRA1 by using the two-hybrid assay and also confirmed the direct interaction between GRL and ATSRA1 (Figure 4B, lower). Therefore, the plant and human NAP125 homologs retain the structural domains that are required for the interaction with ATSRA1.

The only known function of NAP125 is to regulate WAVE complex assembly [2, 20] and ARP2/3-dependent morphogenesis [7, 8, 22, 23]. We tested the ability of human *NAP125* to provide *GRL* function in vivo by over-expressing the human gene in the *grl* background. In all cases, transformed *grl* lines that overexpressed human *NAP125* had highly polarized trichomes (Figure 4C) and epidermal cell-cell contacts that were indistinguishable

from the wild-type (data not shown). The simplest explanation of the rescue result is that human NAP125 functions as an ATSRA1 binding WAVE complex subunit in *Arabidopsis*; however, it remains to be proven that *GRL* functions in the context of a WAVE complex.

The array of *grl* phenotypes is identical to *ARP2/3* subunit mutants [9–13] and suggests that *GRL* positively regulates *ARP2/3*. As an initial test of this idea, we wanted to determine if the actin cytoskeleton in *grl* alleles resembled that of *ARP2/3* subunit mutants. In other genetic or reverse genetic systems, mutations in WAVE subunits have different effects on actin. In *Dictyostelium*, *pirA* (*sra1*) mutant strains have enlarged pseudopods
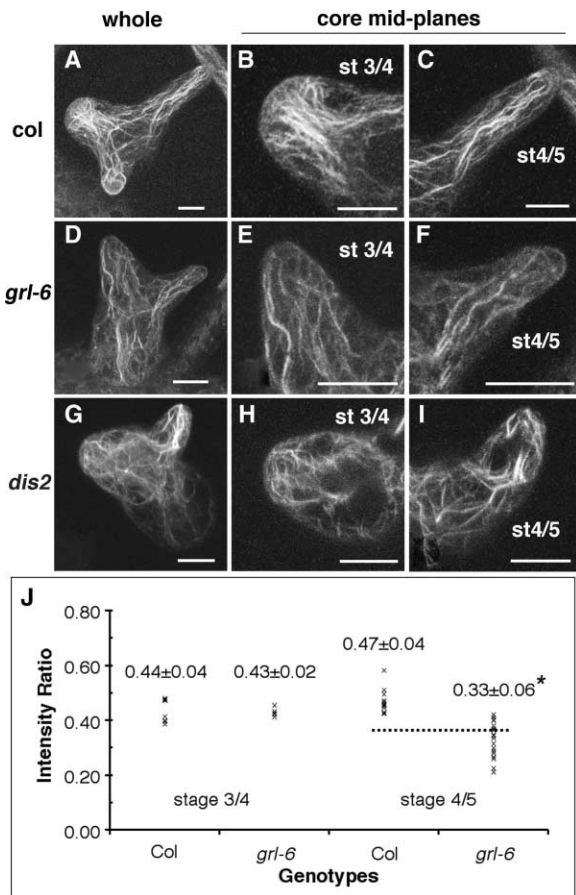
Figure 5. Localization and Quantitation of F-actin in Wild-Type and *grl-6* Trichomes

(A–F) Phalloidin labeling of actin in whole-mounted stage-four trichomes. (A), (D), and (G) are maximum projections of confocal optical sections that include the entire cell. (B), (E), and (H) maximum projections of the core cytoplasm from stage-three/four branches. (C), (F), and (I) maximum projections of the core cytoplasm of stage-four/five branches. (A–C) Col-0 stage-four trichome. (D–F) *grl-6* stage-four trichome. (G–I) *dis2-1* stage-four trichome. (J) Quantitation of the relative amounts of core actin filaments in stage-three/four and stage-four/five branches. The images for (A–I) were obtained from fixed, whole-mounted samples that were probed with Alexa488 phalloidin as previously described [9]. The intensity ratio is expressed as a mean ± SD for all genotypes and branch stages. Asterisk (*), a two-tailed t test showed that the mean intensity ratio for *grl* stage-four/five trichomes was significantly different than the wild-type (p < 0.001). For detailed methods see Supplemental Data.

and increased amounts of F-actin that is concentrated within cell protrusions [6]. Cultured insect cells in which WAVE complex function has been attenuated by RNA interference fail to generate lamellipodia and have reduced localization of F-actin at the cell cortex [7, 8]. The reasons for these discrepancies are not known but may have to do with cell-type-specific differences in WAVE subunit function and/or regulation [24]. We concentrated our actin localization efforts on stage-four cells because the first signs of stalk and branch swelling occur after branch initiation. As previously shown [16], 92% (n = 12 branches) of wild-type stage-four branches contained core cytoplasmic bundles that were loosely aligned with the long axis of the branch (Figures 5A–5C).

In contrast, the actin bundles in similarly staged *distorted1* (*arp3*) and *dis2* (*arpc2*) trichomes are disorganized, and as the branches elongate to 16–50 μm in length, the relative amount of core actin filaments is significantly reduced compared to the wild-type [9, 13]. In a set of control experiments, we confirmed that only 20% (n = 10) of *dis2* (*arpc2*) stage-four branches had aligned core bundles. A representative example of the altered actin organization in young *dis2* (*arpc2*) trichomes is shown in Figures 5G–5I. The branches of *grl* trichomes had intermediate core bundle defects compared to *dis2* and the wild-type. We found that 61% (n = 18) of *grl-T2* and 57% (n = 15) of *grl-6* stage-four branches contained a population of aligned core bundles. The *grl* bundles resembled those of the wild-type but usually did not extend fully toward the branch apex (Figures 5D–5F).

In our localization experiments involving *grl* trichomes, we did not find regions of increased phalloidin fluorescence that could reflect ectopic actin polymerization in *grl* trichomes. In order to compare directly the amount of F-actin in the core cytoplasm of wild-type and mutant branches, we counted the number of phalloidin-positive actin filaments and/or bundles ≥5 μm in length. Wild-type branches contained 6.1 ± 1.4 (n = 12) actin filaments and/or bundles, while *dis2* and *grl* branches contained 2.7 ± 2.4 (n = 10) and 4.7 ± 1.3 (n = 14), respectively. Like *ARP2/3* subunit mutants [9, 13], the core bundles that were present in *grl-6* branches were unstable, because in more elongated stage-four/five branches the relative amounts of core actin bundles was reduced significantly compared to wild-type controls (Figure 5J).

The failure to generate and maintain a normal organization of the actin cytokeleton in *grl* trichomes may reflect the failure to stabilize and/or localize properly a SCAR/WAVE-like ARP2/3 activator. It is also possible that unknown ARP2/3 activators regulate core bundle formation in a *GRL*-independent manner. In this case the core bundle phenotypes in *grl* branches could be caused by an indirect effect of altered actin polymerization elsewhere in the cell. We are in the process of developing probes to simultaneously label actin, ARP2/3 subunits, and GRL in developing trichomes. These tools will help resolve many unanswered questions regarding GRL and ARP2/3 function.

In this paper we report genetic and biochemical evidence that support the utility of the distorted mutants to understand the function and regulation of ARP2/3 during epidermal development. The similar cell shape and actin phenotypes of *grl* and *ARP2/3* subunit mutants suggest that *GRL* positively regulates *ARP2/3*. Based on the physical interaction of GRL with ATSRA1, we hypothesize that these putative WAVE complex subunits are required to transmit activating signals to ARP2/3. The homologous functions of plant and human NAP125 suggest that the subunits share the structural features that are required to couple RHO-GTPase binding with conformational changes in the WAVE complex that affect localization. The RHO-GTPase binding activity of ATSRA1 and the trichome distortion caused by mutations in *ATSRA1* (D. Basu and D.B.S., unpublished data) are consistent with this idea. Therefore, new knowledge

that pertains to *GRL* and *ATSRA1* will have a general relevance to the field of WAVE complex signaling and morphogenesis. Despite the similarities between a subset of the human and plant WAVE subunits, we expect the WAVE and ARP2/3 complexes to have unique functions in plant cells. Unlike the embryo lethality caused by WAVE subunit mutations in *C. elegans* [22] and *Drosophila* [23], *Arabidopsis* plants that carry comparable mutations in *GRL* are slightly stunted but fertile. This result suggests that rather than providing the driving force for cell expansion at the plasma membrane, *GRL* may regulate organelle positioning or intracellular trafficking in novel ways. It will be interesting to find out how directly the rules of *GRL*-dependent morphogenesis transfer from trichomes to other cell types and species.

Supplemental Data
Supplemental Data including Experimental Procedures, four figures, and one table are available at http://www.current-biology.com/cgi/content/full/14/15/1405/DC1/.

References

1. Eden, S., Rohatgi, R., Podtelejnikov, A.V., Mann, M., and Kirschner, M.W. (2002). Mechanism of regulation of WAVE1-induced actin nucleation by Rac1 and Nck. Nature *418*, 790–793.
2. Innocenti, M., Zucconi, A., Disanza, A., Frittoli, E., Areces, L., Steffen, A., Stradal, T.E.B., Di Fiore, P.P., Carlier, M., and Scita, G. (2004). Abi1 is essential for the formation and activation of a WAVE2 signaling complex mediating Rac-dependent actin remodeling. Nat. Cell Biol. *6*, 319–327.
3. Steffen, A., Rottner, K., Ehinger, J., Innocenti, M., Scita, G., Wehland, J., and Stradal, T.E.B. (2004). Sra-1 and Nap1 link Rac to actin assembly driving lamellipodia formation. EMBO J. *23*, 749–759.
4. Machesky, L., and Insall, R. (1998). Scar1 and the related Wiskott-Aldrich syndrome protein, WASP, regulate the actin cytoskeleton through the Arp 2/3 complex. Curr. Biol. *8*, 1347–1356.
5. Machesky, L.M., Mullins, R.D., Higgs, H.N., Kaiser, D.A., Blanchoin, L., May, R.C., Hall, M.E., and Pollard, T.D. (1999). Scar, a WASp-related protein, activates nucleation of actin filaments by the Arp 2/3 complex. Proc. Natl. Acad. Sci. USA *96*, 3739–3744.
6. Blagg, S.L., Stewart, M., Sambles, C., and Insall, R.H. (2003). PIR121 regulates pseudopod dynamics and SCAR activity in *Dictyostelium*. Curr. Biol. *13*, 1480–1487.
7. Rogers, S.L., Wiedemann, U., Stuurman, N., and Vale, R.D. (2003). Molecular requirements for actin-based lamella formation in *Drosophila* S2 cells. J. Cell Biol. *162*, 1079–1088.
8. Kunda, P., Craig, G., Dominguez, V., and Baum, B. (2003). Abi, Sra1, and Kette control the stability and localization of SCAR/

WAVE to regulate the formation of actin-based protrusions. Curr. Biol. *13*, 1867–1875.
9. Le, J., El-Assal, S.E., Basu, D., Saad, M.E., and Szymanksi, D.B. (2003). Requirements for *Arabidopsis ATARP2* and *ATARP3* during epidermal development. Curr. Biol. *13*, 1341–1347.
10. Li, S., Blanchoin, L., Yang, Z., and Lord, E.M. (2003). The putative Arabidopsis Arp2/3 complex controls leaf cell morphogenesis. Plant Physiol. *132*, 2034–2044.
11. Mathur, J., Mathur, N., Kirik, V., Kernebeck, B., Srinivas, B.P., and Hulskamp, M. (2003). *Arabidopsis CROOKED* encodes for the smallest subunit of the ARP2/3 complex and controls cell shape by region specific fine F-actin formation. Development *130*, 3137–3146.
12. Mathur, J., Mathur, N., Kernebeck, B., and Hulskamp, M. (2003). Mutations in actin-related proteins 2 and 3 affect cell shape development in Arabidopsis. Plant Cell *15*, 1632–1645.
13. El-Assal, S.E., Le, J., Basu, D., Mallery, E.L., and Szymanksi, D.B. (2004). *DISTORTED2* encodes an ARPC2 subunit of the putative Arabidopsis ARP2/3 complex. Plant J. *38*, 526–538.
14. Beilstein, M., and Szymanski, D. (2004). Cytoskeletal requirements during *Arabidopsis* trichome development. In The Plant Cytoskeleton in Cell Differentiation and Development, P. Hussey, ed. (Oxford: Blackwell), pp. 265–289.
15. Hulskamp, M., Misra, S., and Jürgens, G. (1994). Genetic dissection of trichome cell development in *Arabidopsis*. Cell *76*, 555–566.
16. Szymanski, D.B., Marks, M.D., and Wick, S.M. (1999). Organized F-actin is essential for normal trichome morphogenesis in *Arabidopsis*. Plant Cell *11*, 2331–2347.
17. Alonso, J.M., Stepanova, A.N., Leisse, T.J., Kim, C.J., Chen, H., Shinn, P., Stevenson, D.K., Zimmerman, J., Barajas, P., Cheuk, R., et al. (2003). Genome-wide insertional mutagenesis of *Arabidopsis* thaliana. Science *301*, 653–657.
18. Kobayashi, K., Kuroda, S., Fukata, M., Nakamura, T., Nagase, T., Nomura, N., Matsuura, Y., Yoshida-Kubomura, N., Iwamatsu, A., and Kaibuchi, K. (1998). p140SRA1 (specifically Rac1-associated protein) is a novel specific target for Rac1 small GTPase. J. Biol. Chem. *273*, 291–295.
19. Frank, M.J., and Smith, L.G. (2002). A small, novel protein highly conserved in plants and animals promotes the polarized growth and division of maize leaf epidermal cells. Curr. Biol. *12*, 849–853.
20. Gautreau, A., Ho, H.Y., Steen, H., Gygi, S.P., and Kirschner, M.W. (2004). Purification and architecture of the ubiquitous Wave complex. Proc. Natl. Acad. Sci. USA *101*, 4379–4383.
21. Kitamura, T., Kitamura, Y., Yonezawa, K., Totty, N.F., Gout, I., Hara, K., Waterfield, M.D., Sakaue, M., Ogawa, W., and Kasuga, M. (1996). Molecular cloning of p125[Nap1], a protein that associates with an SH3 domain of Nck. Biochem. Biophys. Res. Commun. *219*, 509–514.
22. Soto, M.C., Qadota, H., Kasuya, K., Inoue, M., Tsuboi, D., Mello, C.C., and Kaibuchi, K. (2002). The GEX-2 and GEX-3 proteins are required for tissue morphogenesis and cell migrations in *C. elegans*. Genes Dev. *16*, 620–632.
23. Bogdan, S., and Klambt, C. (2003). Kette regulates actin dynamics and genetically interacts with Wave and Wasp. Development *130*, 4427–4437.
24. Blagg, S.L., and Insall, R.H. (2004). Solving the WAVE function. Nat. Cell Biol. *6*, 279–281.

Accession Numbers

The GenBank accession number for the 5′UTR of the GRL mRNA is AY662956.

Note Added in Proof

While this work was under review, our recent finding that *ATSRA1* corresponds to the "distorted group" gene *PIROGI* was accepted for publication in Development. Basu, D., El-Assal, S.E., Le, J., Mallery, E.L., and Szymanksi, D.B. (2004). Interchangeable functions of Arabidopsis PIROGI and the human WAVE complex subunit SRA1 during leaf epidermal morphogenesis. Development, in press.